Ecology, 75(1), 1994, pp. 134–150

CARBON DIOXIDE EXCHANGE BETWEEN AN UNDISTURBED OLD-GROWTH TEMPERATE FOREST AND THE ATMOSPHERE[1]

D. Y. HOLLINGER,[2] F. M. KELLIHER, J. N. BYERS, J. E. HUNT,
T. M. MCSEVENY, AND P. L. WEIR
Landcare Research New Zealand, Ltd., P.O. Box 31-011, Christchurch, New Zealand

Abstract. We used the eddy-correlation technique to investigate the exchange of CO_2 between an undisturbed old-growth forest and the atmosphere at a remote Southern Hemisphere site on 15 d between 1989 and 1990. Our goal was to determine how environmental factors regulate ecosystem CO_2 exchange, and to test whether present knowledge of leaf-level processes was sufficient to understand ecosystem-level exchange.

On clear summer days the maximum rate of net ecosystem CO_2 uptake exceeded 15 $\mu mol \cdot m^{-2} \cdot s^{-1}$, about an order of magnitude greater than the maximum values observed on sunny days in the winter. Mean nighttime respiration rates varied between ≈ -2 and -7 $\mu mol \cdot m^{-2} \cdot s^{-1}$. Nighttime CO_2 efflux rate roughly doubled with a 10°C increase in temperature.

Daytime variation in net ecosystem CO_2 exchange rate was primarily associated with changes in total photosynthetically active photon flux density (PPFD). Air temperature, saturation deficit, and the diffuse PPFD were of lesser, but still significant, influence. These results are in broad agreement with expectations based on the biochemistry of leaf gas exchange and penetration of radiation through a canopy. However, at night, the short-term exchange of CO_2 between the forest and the atmosphere appeared to be regulated principally by atmospheric transport processes. There was a positive linear relationship between nocturnal CO_2 exchange rate and downward sensible heat flux density. This new result has implications for the development of models for diurnal ecosystem CO_2 exchange.

The daytime light-use efficiency of the ecosystem (CO_2 uptake/incident PPFD) was between 1.6 and 7.1 mmol/mol on clear days in the summer but decreased to 0.8 mmol/mol after frosts on clear winter days. Ecosystem CO_2 uptake was enhanced by diffuse PPFD, a result of potentially global significance given recent increases in Northern Hemisphere haze.

Key words: atmospheric turbulence; canopy; CO_2; CO_2 exchange vs. PPFD; daytime ecosystem light use efficiency; eddy correlation; gas exchange; nocturnal CO_2 flux; Nothofagus; *Southern Hemisphere old-growth forest.*

INTRODUCTION

Direct measurements of plant community carbon dioxide exchange are needed to validate physiologically based modeling efforts that seek to scale from individual leaves to canopies, then to regions. Such measurements are also necessary for resolving questions about the significance and nature of the terrestrial biosphere as a global carbon source or sink, and how this may change in the future. We used the eddy-correlation technique to make area-averaged measurements of net CO_2 exchange between the atmosphere and an undisturbed, old-growth forest at a remote Southern Hemisphere site with the objective of determining how environmental factors regulate these exchanges. We propose that if we are to reliably scale measurements up from the leaf level, we must be able to explain the basic patterns of ecosystem CO_2 exchange according to our present understanding of the biochemistry of leaf gas exchange. Hence we expect ecosystem CO_2 uptake to increase at first rapidly with an increasing photosynthetically active photon flux density (PPFD), and then more slowly at higher PPFDs as leaf-level photosynthesis saturates. Similarly, we expect daytime ecosystem CO_2 uptake and nighttime respiration to follow the functional responses of leaf photosynthesis and respiration to temperature.

Understanding how individual elements (e.g., leaves) are put together in a canopy should also provide insight into properties that may emerge collectively at the stand level but either do not exist or are unimportant at the leaf level. Divergence of stand level responses to environmental variables from those at the leaf level may be indicative of these new or "emergent" properties. Finally, we propose that knowledge of ecosystem organization and temporal changes in ecosystem properties (e.g., leaf area index) should also provide testable hypotheses about stand carbon exchange. We briefly discuss general features of leaf gas exchange and use models that reproduce these features to examine our measurements of forest CO_2 exchange.

[1] Manuscript received 31 July 1992; revised and accepted 5 April 1993.

[2] Present address: U.S. Forest Service, Northeastern Forest Experiment Station, P.O. Box 640, Durham, New Hampshire 03824 USA.

Leaf and tissue gas exchange

Carbon dioxide uptake by an ecosystem is the result of the biochemical reactions of photosynthetic carbon fixation. Ecosystem respiration is similarly the sum total of respiratory processes in leaves, stems, roots, other plant parts, and soil heterotrophs. The balance between the photosynthetic (P) and respiratory (R_x) processes determines whether the ecosystem is gaining or losing carbon and is termed net ecosystem exchange (NEE):

$$\text{NEE} = \Sigma P - \Sigma R_{\text{leaves}} - \Sigma R_{\text{stems}} - \Sigma R_{\text{roots}} - \Sigma R_{\text{soil}}. \quad (1)$$

The saturating response of leaf photosynthesis to light is understood and modeled at the biochemical level as the transition from a limitation in ribulose-1,5-bisphosphate (RuP_2) regeneration associated with insufficient energy for electron transport/photophosphorylation at low PPFD to a limitation caused by insufficient RuP_2 carboxylation capacity at high PPFD (Farquhar et al. 1980). Additional biochemical limitations on carboxylation have been considered in more recent versions of Farquhar's model (e.g., Kirschbaum and Farquhar 1984, Collatz et al. 1991). Simple empirical models can reproduce the saturating behavior of photosynthesis to light. We employ two of these (Michaelis–Menten enzyme kinetics and an exponential relationship) that accurately simulate the functional response of leaf-level photosynthesis to PPFD (but not the biochemistry) to address our hypothesis that leaf-level responses will be seen in canopy-scale measurements.

Michaelis–Menten kinetics describe the basic form of the photosynthetic light response as:

$$P = P_{\text{max1}} \cdot I/(K_m + I) - R_d, \quad (2)$$

where P_{max1} is a maximum rate of photosynthesis, I is the light intensity, K_m the Michaelis–Menten constant (PPFD at which P is one half of P_{max1}), and R_d is a respiratory term. Landsberg (1977) modeled the light response of photosynthesis as:

$$P = P_{\text{max2}} \cdot (1 - e^{-\alpha \cdot (\text{PPFD} - I_{\text{comp}})}), \quad (3)$$

where P_{max2} is a maximum rate of photosynthesis, α is a curve "shape" factor, and I_{comp} is the light compensation point.

In many species leaf photosynthesis has been observed to reach a maximum between 15 and 30°C. This results from the differential effect of temperature on the K_ms of RuP_2 carboxylase-oxygenase for carbon dioxide and oxygen (Berry and Raison 1981) and the temperature response of dark respiration. We used a quadratic relationship to examine the ecosystem CO_2 exchange data for evidence of a temperature optimum.

Dark respiration (R) increases approximately exponentially with the inverse of the absolute temperature as:

$$R = \beta \cdot e^{-E_a/G \cdot T}, \quad (4)$$

where β is a nonexponential term that may or may not depend on temperature, E_a is the activation energy of the reaction (in joules per mol), G is the universal gas constant (8.3 $J \cdot mol^{-1} \cdot K^{-1}$), and T is the temperature (in kelvins, K). E_a/G can be thought of as the "temperature" at which respiration occurs at 37% ($1/e$) of its maximum possible rate (Berry and Raison 1981).

Photosynthesis is also affected by other factors, including air saturation deficit (D), and water stress. These can indirectly affect photosynthetic performance by reducing stomatal aperture (Morison 1987), which results in reduced CO_2 concentrations at the sites of enzyme activity and lower CO_2 fixation. There may also be direct effects of saturation deficit and water stress on photosynthetic mechanisms (e.g., Schulze 1986).

Methods

Experimental site

Data were collected between July 1989 and March 1990 in virgin *Nothofagus* forest near the township of Maruia in the South Island, New Zealand (42°12′ S, 172°15′ E; 400 m above sea level). The experimental site was on a glacial terrace in moderately complex terrain (Fig. 1). Predominant daytime winds during observations and throughout the year were from the northwest and southwest with a fetch of ≈1 km. At night, katabatic winds predominate as air drains down the valley from the southeast, with a forested fetch of >10 km.

Vegetation was dominated by emergent *Nothofagus fusca* (red beech) with a subcanopy of *N. menziesii* (silver beech). This temperate, broadleaved evergreen forest is ≈30 m tall with a 10 m canopy depth. Most emergent trees were >1 m diameter and at least 300 yr old. Patches of forests to the east of our site were cut at various times between 1970 and 1980, and are now vigorously regenerating in red and silver beech and other species (*Rubus fruticosus, Leyceteria formosa, Pteridium esculentum*). Forest–scrub boundaries lie ≈900 m to the southwest and 1000 m to the northwest of our point of measurement. Stand characteristics were measured in a 60 × 60 m plot surrounding our instrumented tower. Information about the size and age structure, development, and stand dynamics of this forest have been published previously (Stewart and Rose 1990, Stewart et al. 1991).

The root zone was generally <0.5 m deep and comprised 0.05–0.1 m of forest floor overlying sandy loam soil with ≈25% volumetric coarse fragment content. The forest floor alone had an available water storage capacity of ≈40 mm. Because there are ≈200 rain-days per year at the site, trees experienced minimal water stress.

The leaf area index (LAI) of the stand was estimated from litterfall data. Leaf litter was collected at approximately monthly intervals from 14 collectors located

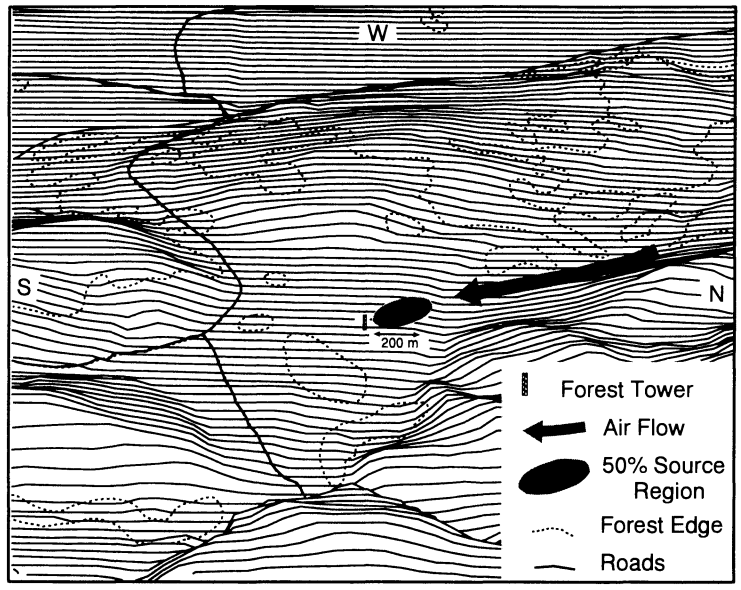

FIG. 1. Forest study site viewed from the east. Predominant daytime winds travel up the valleys from the northwest (arrow) or southwest. The ellipse indicates a typical source region (50% isopleth) for the measured canopy gas exchange. The hill to the west of the tower rises ≈80 m from the valley floor.

across a 1-ha plot ≈100 m from the tower. Each collector had a diameter of 0.74 m. Leaves were dried, separated by species, and then weighed. The area of the fallen leaves was determined each month by measuring the area of a subsample of leaves of each species with a video leaf area meter (model AMS, Delta-T Devices, Cambridge, England), weighing the subsamples to obtain an area per unit mass, and then multiplying by the total leaf dry mass of each species. Leaf shrinkage during senescence was estimated by measuring the leaf area of 20 attached red beech leaves and remeasuring them again after abscission. Leaf shrinkage averaged 13%, so dry leaf area was multiplied by 1.15 to calculate live leaf area. The production of new leaves was determined by measuring the extension of 40 twigs. The proportion of the total leaf area produced at any date was assumed to be equal to the measured proportion of total seasonal twig extension.

Instrumentation

A 32 m tall scaffolding tower was erected, without removing any trees, to allow access through and above the canopy. This tower was instrumented for background micrometeorological measurements and used as a platform for the flux measurement instrumentation during a series of intensive field studies.

We continuously measured total and diffuse photosynthetically active photon flux density (PPFD), rainfall, wind speed, wind direction, air temperature, and humidity above the forest at 32 m, and soil temperature at a depth of 0.1 m. Signals from the instruments were measured at 3-s intervals and stored as 30-min averages on a data logger (model CR10, Campbell Scientific, Logan, Utah, USA).

During intensive field studies this instrumentation (except that for diffuse PPFD and rainfall) was duplicated, with additional measurements of net and total radiation (model CN1 net radiometer, Carter-Scott Design, Fairfield, Victoria, Australia; model 8-48 radiometer, The Eppley Laboratory, Newport, Rhode Island, USA) and forest-floor heat-flux density (Kelliher et al. 1992).

We measured CO_2, water vapor, and sensible heat with eddy-correlation instruments mounted on a pole above the tower at a height of 36 m above the forest floor. These were a three-dimensional (3-D) sonic anemometer (model SWS-11 with a model 3KE head, Applied Technology, Boulder, Colorado, USA), and a Krypton-line ultraviolet hygrometer (model KH2O, Campbell Scientific, Logan, Utah, USA). The measurements of water vapor and heat flux were used to evaluate the site energy balance (data not reported here) and to correct the CO_2 flux measurements. The instruments were mounted on a boom connected to the pole by an antenna rotator and could be remotely pointed into the prevailing wind. The intake of a polypropylene tube (interior diameter: 4 mm) was located ≈0.2 m from the 3-D anemometer and was used to duct a sample of air to a closed-path nondispersive infrared CO_2 analyzer (model 225 Mk3, Analytical Development Company, Hoddesdon, England) located in a hut at the base of the tower. The analyzer mounting was isolated from the building to prevent vibration affecting the readings. Air was drawn through 40 m of tubing to the hut, then through an 8-μm filter, a heat

exchanger consisting of 5-m coiled copper tubing immersed in water, the analysis cell of the gas analyzer, and then a flow meter at a rate of 4 L/min. The gas analyzer was operated in differential mode, with a trapped sample of ambient air in the reference cell. We also measured the mean half-hourly difference in CO_2 concentration between the sampled gas from 36 m and our trapped air sample. All connections were gas tight, and a vacuum gauge was used to read the gas pressure in the infrared gas analyzer (IRGA) analysis cell (typical pressure drop of ≈ 3 kPa). In this configuration, the analyzer $1 - 1/e$ time constant was 2.2 s, as measured by rapidly switching between two airstreams of different CO_2 concentration with a high-speed solenoid valve.

The instruments were read by a data acquisition system consisting of either a 12 or 16 bit analog to digital board (models DAS 16G or DAS HRES, Metrabyte, Taunton, Massachusetts, USA) and a microcomputer. Raw data values were sampled at 10 Hz and recorded on disk, and half-hourly fluxes were calculated with a computer program written by R. McMillen (1988). All raw data were retained and archived on optical disks (model PC-800, Storage Dimensions, San Jose, California, USA).

The manufacturer's calibration was used for the sonic anemometer. The krypton hygrometer was calibrated by placing a chamber across the gap of the hygrometer and flowing air from a precision water-vapor generator (model WG-600, Analytical Development Company, Hoddesdon, England) through the chamber at 300 mL/min. We generated a very tight ($r^2 > 0.98$) 8–12 point calibration for this instrument every few days while in the field. The slope of these log-linear calibration curves typically changed by <4% over 2 d. The long-term stability of the hygrometer was also good. Over a season, one standard deviation of the calibration slopes was equal to 4% of the mean. The CO_2 analyzer was calibrated with a bottle of reference air that was calibrated in turn with a two-stage cascade of mixing pumps (model SA27/3F, Wösthoff, Bochum, Germany) that combined CO_2-free air and pure (>99.9%) CO_2. Bottle calibration was better than 1%, yielding a similar accuracy in analyzer gain calibration. Over several days of measurement this gain calibration would typically drift by <3%. Zero drift in the CO_2 analyzer and slow changes in ambient CO_2 concentration or pressure have only minimal effects on eddy flux estimates because of the real-time running-mean removal technique used in the flux calculations.

Calculation of CO_2 exchange rates

CO_2 exchange between the forest ecosystem and the atmosphere consists of two components: a turbulent eddy flux transported across the plane of instrumentation above the forest (F_c), and exchange below the instrumentation height, which is manifest as a change in the mean concentration of CO_2 in the forest air column. The net flux of CO_2 crossing the plane at our instrumentation height was calculated as the mean covariance between fluctuations in vertical wind velocity (w) and the density of CO_2 (c) (Baldocchi et al. 1988):

$$F_c = \rho_a \cdot (\overline{w'c'}), \tag{5}$$

where ρ_a is the density of air, the primes denote deviations from the mean, and the overbar signifies a time average. We used an averaging period of 30 min, which corresponds to a sampling error of $\approx 10\%$ (Baldocchi et al. 1988), and adopt an "ecological" convention for our CO_2 measurements where carbon flux into the ecosystem is defined as positive. The flux associated with a change in storage ($F_{\Delta S}$) is calculated as:

$$F_{\Delta S} = \frac{V \cdot \Delta c}{m}, \tag{6}$$

where V is the volume of the air column below the instrumentation height (36 m^3), Δc is the change in CO_2 concentration per unit time, and m is the molar volume of CO_2. In the absence of advection, the daily net storage of CO_2 in the air column is zero. We found in a previous study of *Nothofagus* forest that the half-hourly change in CO_2 concentration throughout a vertical profile in the forest was not significantly different from the half-hourly change in CO_2 concentration above the forest (Fig. 2). We therefore used the half-hourly change in concentration at 36 m as the Δc for our estimates of $F_{\Delta S}$.

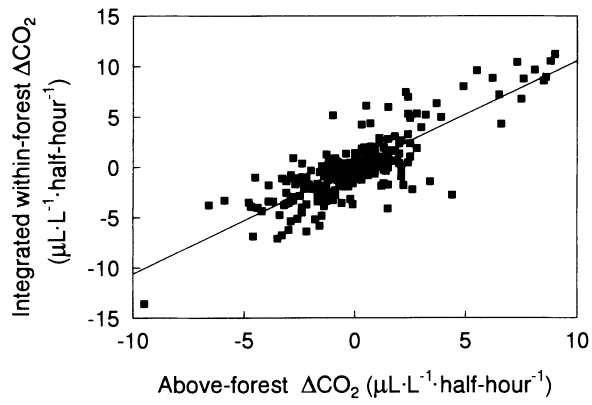

FIG. 2. Relationship between the change in half-hourly CO_2 concentration 4 m above a *Nothofagus* forest (ΔCO_2) and the integrated mean half-hourly change in CO_2 concentration at four levels within the forest (measured at 6, 55, 78, and 100% of canopy height). The slope of the regression line is not significantly different from 1.

The net flux between the ecosystem and atmosphere (F_c) is the sum of the eddy and the Δ-storage fluxes:

$$F_c = F_c + F_{\Delta S}. \tag{7}$$

Eddy flux covariances were computed in real time with a running-mean removal technique based on a digital recursive filter (for details on these computations see Dyer et al. [1967] and McMillen [1988]). The

TABLE 1. Vegetation basal area and frequency in a New Zealand beech forest.

Species	Basal area (m^2/ha)	Frequency (stems/ha)
Red beech	50.5	336
Silver beech	17.1	775
Total	67.7	1111

optimal time constant for the digital filter at our forest site was ≈600 s. A two-angle coordinate rotation was performed on the wind data in the covariance calculations to remove the effects of instrument tilt or terrain irregularity on the airflow (McMillen 1988). We digitally filtered the raw vertical wind-speed values (w) to match the time constant of the CO_2 analyzer because mismatched instrument time-response characteristics can lead to errors in covariances (Businger and Delany 1990). Signals from the sonic anemometer were digitally lagged to remain in phase with the airstream that travelled through tubing to the CO_2 analyzer. The lag was determined by calculating the maximum covariance between the vertical wind speed and the CO_2 concentration, and confirmed by flow-volume calculations and by timing the response of the analyzer to someone blowing into the inlet of the CO_2 tube above the forest.

We used the procedure of Webb et al. (1980) to correct the CO_2 flux measurements for changes in the density of air associated with changes in the water-vapor content. Our CO_2 inlet tube heat exchanger eliminated the need for the larger corrections associated with changes in air temperature. Additional corrections were applied to the CO_2 flux estimates to account for the incomplete spectral response of our CO_2 analyzer, sensor separation, signal processing (Moore 1986), the cross sensitivity of our analyzer to water vapor, and the damping effect on CO_2 fluctuations of the inlet tube to our analyzer (Leuning and Moncrieff 1990). Most of the time these corrections were individually of the order ±10%.

We estimated the dimensions of the flux source area or "footprint" with the statistical source area model of Schmid and Oke (1990). We assessed the validity of the site for making eddy flux measurements by evaluating the energy balance and calculating turbulence spectra and cospectra. The energy balance was calculated as:

$$R_n - J - S = H + \lambda E, \quad (8)$$

where R_n was the measured net radiation, J was the estimated tree-canopy energy storage rate, S was the measured forest-floor heat-flux density, and H and λE were the sensible and latent heat-flux densities, respectively, measured with the eddy flux system. Details of the beech forest energy balance measurements are presented in Kelliher et al. (1992).

We computed turbulence spectra and cospectra by fast Fourier transform using a program written by Carter and Ferrie (1979). Spectra were computed from twelve series of 8192 data points that had been recorded at 10 Hz. Coordinates were rotated in two dimensions to force the mean vertical (w) and lateral (v) wind velocities to zero. Each time series was tapered with a cosine window and linear trends were removed. The raw estimates were logarithmically blocked to produce individual spectra that were normalized by their variance. Twelve spectra were averaged by frequency to produce the final spectra.

We explored the hypothesis that, for the purposes of understanding net ecosystem CO_2 exchange, the ecosystem can be profitably treated as a "big leaf" by determining how well simple models that mimic the response of leaf-level CO_2 exchange fit whole-ecosystem CO_2 exchange. We used Eqs. 2 and 3 to model the response of CO_2 exchange to PPFD, a quadratic temperature relationship, and a linear model to relate CO_2 exchange and D. For each measurement period we subtracted the best-fitting model from the measured flux values and tested whether the residual variation in CO_2 flux was related to variation in other environmental factors.

RESULTS

Forest stand and environment

Basal area at the study site was dominated by red beech (Table 1) although silver beech trees are more frequent than red beech. Dominant trees at the site were >1 m in diameter, with a maximum age of >400 yr. Beech leaves are held in the canopy for ≈15 mo. As a result, the projected area of foliage per unit of ground area (LAI) varies seasonally from a low of ≈5 in midwinter (July) to just over 7 in midsummer (February–March) (Fig. 3). Our measurements in December (late spring) were made while the new leaves of both beech species were expanding. Red beech foliage comprised on average about 90% of the LAI and 85% of the foliage biomass.

The mean annual air temperature at the site between 1988 and 1991 was 10.1°C. The mean temperature of the warmest month (January) was 16.3°C and the mean temperature of the coolest month (July) was 3.0°C. Absolute maxima and minima during this time were 31.9° and −7.2°C, although temperatures never remained below zero throughout an entire day. Annual precipitation averaged 2035 mm, with no month receiving <32 mm. Clouds were frequent at the site, with rain falling on ≈200 d/yr. The mean day and night wind speeds at 32 m were 1.6 and 1.2 m/s, respectively.

The total photosynthetically active photon flux density (PPFD) reaching the forest in 1989 was ≈9400 mol/m^2. Approximately 40% of this flux was diffuse (cloud plus sky light). Because of the frequent cloudiness, most daylight hours in 1989 (defined as PPFD

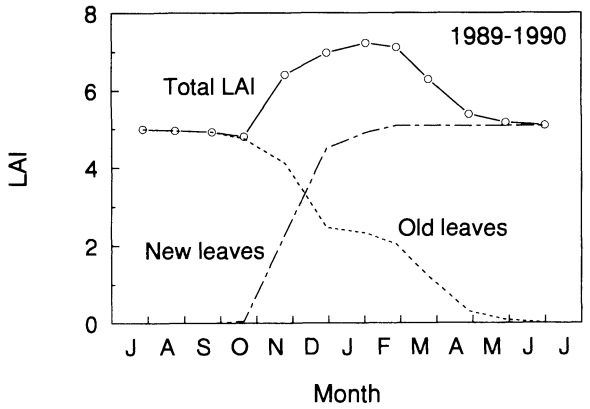

FIG. 3. Seasonal pattern of leaf area index (LAI) in a New Zealand *Nothofagus* forest. Leaves are held in the canopy for 12–15 mo so that LAI reaches a maximum during the summer (December–March).

>50 μmol·m^{-2}·s^{-1}) had a high component of diffuse PPFD; during 49% of the daylight hours more than 2/3 of the total PPFD was diffuse, and during another 23% the diffuse fraction ranged between 1/3 and 2/3.

Suitability of site for eddy flux measurements

We obtained energy balance closure to within 5% at our site when eddy-correlation-derived measurements of H (sensible heat flux density) and λE (latent heat flux density) were compared to $R_n - J - S$ (measured net radiation minus estimated tree-canopy storage rate minus measured forest-floor heat-flux density) for both half-hourly and daily integration periods (Kelliher et al. 1992). Differences were larger during periods of intermittent cloudiness, which reflected differences in the sampling areas between $(H + \lambda E)$ and $(R_n - J - S)$ in a variable radiation regime. Eddy fluxes of water vapor measured at our site also agreed with the sum of tree transpiration measured with a heat flow method and forest-floor evaporation measured with mini-lysimeters (Kelliher et al. 1992, Köstner et al. 1992).

Power spectra of the fluctuations of vertical wind speed, temperature, water vapor density, and CO_2 density depict the turbulent behavior of the atmosphere filtered by the frequency response characteristics of the instrumentation. The response of our wind and temperature sensors were near ideal, and when plotted along nondimensional surface coordinates, power spectra of the turbulent fluctuations of vertical windspeed (w) and temperature (T) obtained at our site (Fig. 4) were similar to results first obtained over a flat landscape (Kaimal et al. 1972) and later extended to crop surfaces and forests (e.g., Anderson and Verma 1985, Ohtaki 1985, Anderson et al. 1986). These later studies showed that water vapor and CO_2 density fluctuations obeyed the same scaling laws as the fluctuations in vertical wind speed and temperature, and that their spectra were similar in shape to the w and T curves. Our power spectra of water-vapor density fluctuations (q) were similar to those of w and T at the lower frequencies, but showed the influence of instrumental noise in the change of slope at higher frequencies (Fig. 4). A slope of $+1$ is typical of white noise in a log–log plot of spectral power vs. frequency (Wesely and Hart 1985). White noise should not significantly affect the accuracy of flux measurements as long as the noise is not correlated with fluctuations in the vertical wind velocity, but it will lower the measurement precision (Wesely and Hart 1985). We expected that the response characteristics of our CO_2 analyzer would prevent us from measuring high-frequency changes in CO_2 density. The CO_2 power spectra (Fig. 4) showed the expected roll-off at higher frequencies caused by the slow analyzer response, as well as some high-frequency noise. An ideal CO_2 analyzer would have tracked the high-frequency response of wind and temperature fluctuations.

The total eddy flux is equal to the integral of the cospectra of w and the entity of interest for all frequencies (the area under the curves in Fig. 5). The general shape, frequency of peak flux, and high-frequency roll-off of the cospectra of sensible (wT) and latent (wq) heat fluxes (Fig. 5A) were similar to those recorded previously over forest for unstable conditions (Anderson et al. 1986). The noise from the hygrometer is seen in the greater scatter at the higher nondimensional frequencies of the cospectra. The drop-off at higher frequencies in the cospectra of the fluctuations in vertical wind speed and CO_2 (wc) compared to the cospectra of w and T at our site represented 5–15% of the total flux (especially visible in the log-linear plots in Fig. 5B), similar to values estimated by the procedure of Moore (1986). Under stable atmospheric conditions at night our spectra were more variable but did not show the systematic shift towards higher frequencies suggested by McBean and Miyake (1972) for steady-

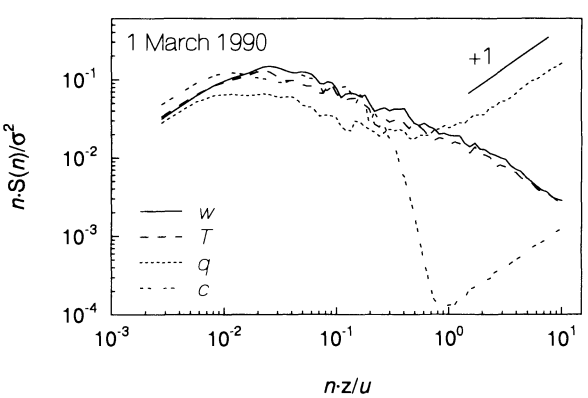

FIG. 4. Power spectra of turbulent fluctuations of vertical wind speed (w), temperature (T), water vapor density (q), and CO_2 density (c). Spectra are normalized in the frequency domain by the product of the frequency (n), the height of the instrumentation above the zero-plane displacement height (z), and the reciprocal of the horizontal wind speed (u). The power is expressed as the product of the frequency and the spectral power at that frequency ($S(n)$), normalized by the variance.

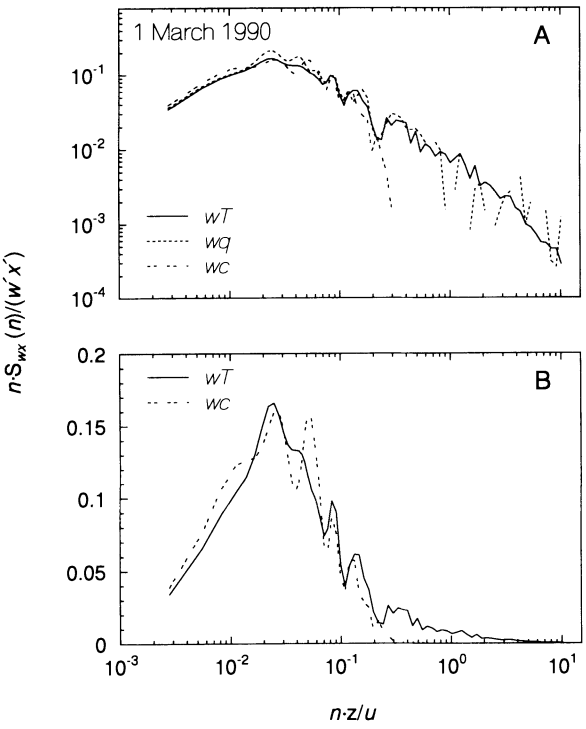

FIG. 5. Cospectra of vertical wind speed and temperature (wT), vertical wind speed and water-vapor density (wq), and vertical wind speed and CO_2 density (wc) on log–log (A) and log-linear (B) plots. Spectra are normalized in the frequency domain as in Fig. 4. The cospectral flux of the vertical wind speed and scalar (wx) is expressed as the product of the frequency (n) and the cospectral power at that frequency ($S_{wx}(n)$), normalized by the covariance.

state conditions. Ohtaki (1984) showed that nighttime CO_2 fluxes are transported by infrequent, sudden, wave-like variations not normally considered as turbulence. We therefore used Moore's frequency corrections derived for unstable conditions for both daytime and nighttime CO_2 fluxes.

Source location of eddy fluxes

The location, dimensions, and area of the source region for the measured fluxes are a function of wind speed, wind direction, instrument measurement height, and atmospheric stability. The source area model of Schmid and Oke (1990) is based on a reverse-plume concept, which treats the surface as a collection of source "plumes." The statistical version of the model yields an elliptical estimate of the source region. This ellipse lengthens with increasing wind speed and contracts with an increase in the sensible heat flux. The width of the ellipse is primarily a function of the variance in the lateral component of the wind field (σv), becoming wider with increasing σv. The location of the ellipse is determined by the mean wind direction.

The 50% isopleth and maximum source location within the ellipse for typical daytime conditions is shown on Fig. 1. The location of the maximum source contribution varied from ≈40 to 150 m upwind of our tower, and the 50% flux area varies on average from ≈2 to 8 ha, representing an integration of the flux exchange characteristics of ≈2000–10 000 trees. At night the source region was typically smaller, and was located to the east of the tower.

The energy balance, stemflow measurements, and spectral data all indicated that the site and instrumentation were suitable for valid determinations of fluxes by the eddy correlation method.

Diurnal patterns of CO_2 exchange

There was a strong diurnal pattern of daytime net forest CO_2 uptake and nighttime respiratory loss at all times of the year (Fig. 6). Maximum rates of uptake were lowest after the freezing nights of winter (July), reaching maximum midday values of only 1–2 μmol·m^{-2}·s^{-1}. Maximum daily CO_2 exchange rates were substantially higher by September, and reached values in late summer (February–March) of ≈20 μmol·m^{-2}·s^{-1}. On a leaf area basis, maximum net CO_2 exchange rates were very low, ranging between ≈0.3 μmol·m^{-2}·s^{-1} in July and ≈3 μmol·m^{-2}·s^{-1} in March.

Nighttime ecosystem respiration followed a similar pattern, with a low in winter of ≈ −2 to −3 μmol·m^{-2}·s^{-1} (negative because the ecosystem is a source of CO_2), and greater (more negative) values in spring and summer (Table 2). In contrast to the pattern of maximum daytime CO_2 uptake, however, nighttime respiration rates reached a maximum of ≈ −7 μmol·m^{-2}·s^{-1} in late spring (December) rather than later in the summer. This was still true when respiration rates were extrapolated to a common temperature of 10°C (Table 2). The period of positive CO_2 uptake by the ecosystem varied roughly with daylength, ranging from a minimum of ≈6 h in July to almost 14 h in January.

Daytime and nighttime eddy flux densities were generally several times larger than the flux associated with a change in the CO_2 concentration in the forest air below 36 m (Fig. 6). Daytime in winter was an exception, as the change in storage flux dominated, indicating that most CO_2 uptake at that time was refixation of the previous night's respiration. This may be because the increased thermal stability of the atmosphere over the forest in winter inhibits mixing of the forest air with that from the atmosphere above.

The flux associated with the changing storage of CO_2 in the air column can be appreciable at certain times of day, especially in the early morning (Fig. 6). The change in storage equated with a flux that peaked around 6 μmol·m^{-2}·s^{-1} by midmorning (1000), dropped away to zero by mid- to late afternoon, and then became negative (indicating the storage of respired CO_2 in the forest air column) overnight. The maximum eddy flux was usually observed around midday. In the early morning, eddy and storage fluxes were sometimes opposite in sign, indicating that photosynthetic CO_2 up-

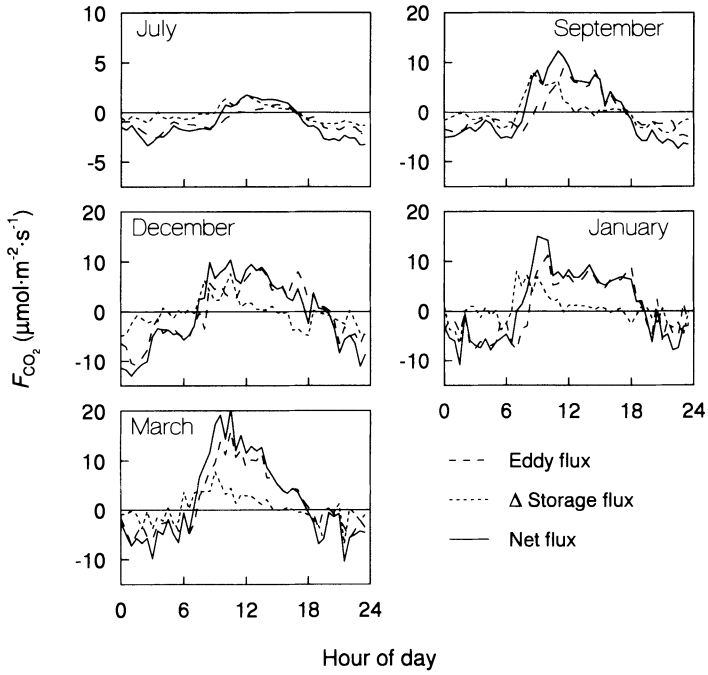

FIG. 6. Seasonal pattern of ecosystem CO_2 exchange (F_{CO_2}) in a remote undisturbed *Nothofagus* forest. Values are half-hourly means for 3 d of each month.

take was taking place while CO_2-enriched air was simultaneously being expelled to the atmosphere above as the nighttime thermal stratification of the air over the forest broke down. At all times of year the peak ecosystem CO_2 uptake occurred by solar noon. The morning increase in CO_2 uptake was generally steeper than the afternoon decline.

Influence of environmental factors on daytime CO_2 exchange

Light.—The photosynthetically active photon flux density (PPFD) was the most important factor regulating daytime ecosystem CO_2 exchange at all times of the year. In the spring and summer, models that incorporated the saturating response of leaf biochemistry provided a better description (higher r^2) of the relationship between above-canopy PPFD and ecosystem CO_2 exchange than a linear model (Fig. 7 and Table 3). Michaelis–Menten (Eq. 2) or Landsberg models (Eq. 3) provided essentially identical fits to the data (Table 3). The nonlinear, least-squares technique for fitting saturating models of photosynthesis to PPFD established values reasonable for leaf-level photosynthesis. Fitted maximum rates of ecosystem CO_2 uptake (P_{max})

TABLE 2. Seasonal characteristics of a New Zealand beech forest CO_2 exchange. PPFD = photosynthetically active photon flux density.

	Winter (July)		Early spring (September)		Late spring (December)		Summer (January)		Late summer (March)	
Season	Mean	SD	Mean	SD	Mean	SD	Mean	SD	Mean	SD
Mean midday PPFD (μmol·m^{-2}·s^{-1})	931	13	1450	200	1856	436	1897	438	1451	236
Mean midday T_{air} (°C)	5.8	1.0	14.9	1.9	18.0	2.9	19.6	5.3	18.6	2.3
Midday net CO_2 uptake† (μmol·m^{-2}·s^{-1})	1.6	0.4	7.6	3.2	6.7	4.9	8.4	4.9	12.9	6.1
Mean night air temperature (°C)	−3.1	1.8	5.7	1.7	8.0	2.9	9.5	3.4	9.7	2.4
Mean night soil temperature (°C)	4.1	0.8	8.4	1.1	12.7	0.9	14.4	1.2	14.1	1.0
Nighttime respiration (μmol·m^{-2}·s^{-1})	−2.4	1.1	−4.5	3.2	−6.7	6.4	−5.2	6.1	−5.0	5.1
Nighttime respiration at 10°C (μmol·m^{-2}·s^{-1})	−4.8		−5.6		−6.6		−4.6		−4.5	

† PPFD > 1000 μmol·m^{-2}·s^{-1}, except July PPFD > 900 μmol·m^{-2}·s^{-1}.

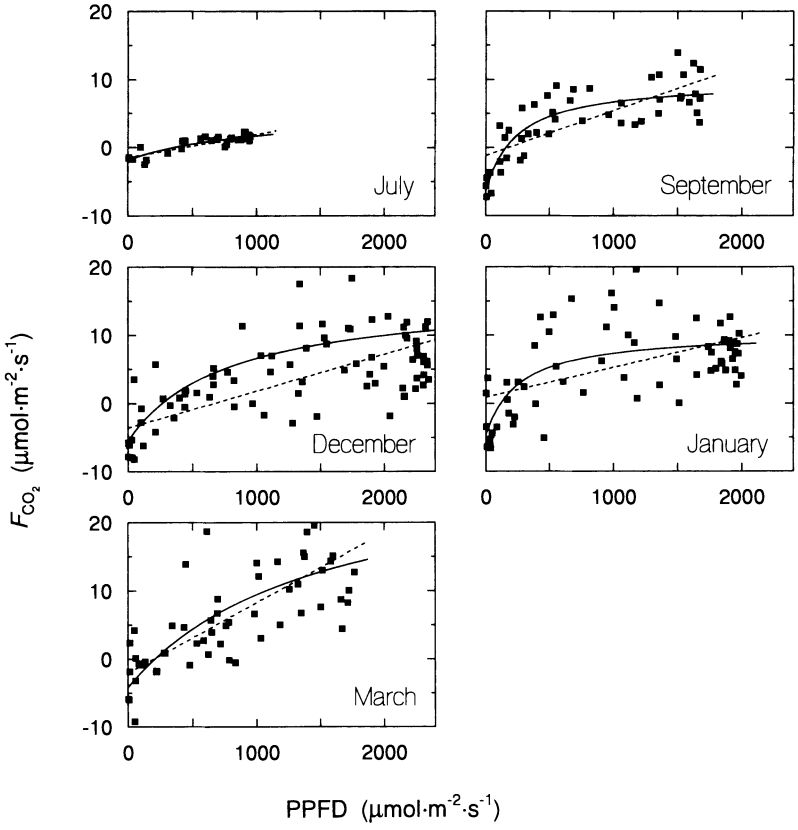

FIG. 7. Relationship between net ecosystem CO_2 exchange (F_{CO_2}) and PPFD at different times of the year. The best-fit linear (– – –) and saturating models (——) are shown for each period. The fitted Michaelis–Menten and Landsberg models produce curves that are indistinguishable.

varied more than four-fold between winter (July) and late summer (March), and other fitted parameters also varied through the year (Table 3). The dark respiration values obtained from fitting daytime data to the saturating models (Table 3) agreed reasonably well with the measured nighttime respiration rates (Table 2).

The initial slope (0–500 μmol·m^{-2}·s^{-1}) of the relationship between net ecosystem CO_2 uptake and

TABLE 3. Relationship between CO_2 exchange and half-hourly PPFD.

Season	Winter (July)	Early spring (September)	Late spring (December)	Summer (January)	Late summer (March)
			Saturating models		
1) Michaelis–Menten					
P_{max1} (CO_2 uptake, μmol·m^{-2}·s^{-1})	7.2	16.1	21.6	14.2	31.1
K_m (PPFD, μmol·m^{-2}·s^{-1})	1020	245	762	327	1368
R_d (CO_2 release, μmol·m^{-2}·s^{-1})	−1.9	−6.2	−5.5	−4.5	−4.1
r^2	0.77	0.75	0.67	0.44	0.58
2) Landsberg					
P_{max2} (CO_2 uptake, μmol·m^{-2}·s^{-1})	2.6	7.5	13.2	8.0	17.0
α (nondimensional)	0.0015	0.0033	0.0008	0.0033	0.0010
I_{comp} (PPFD, μmol·m^{-2}·s^{-1})	354	173	221	137	215
r^2	0.77	0.74	0.65	0.46	0.58
			Linear models		
Initial slope† (CO_2/PPFD, μmol/μmol)	0.0059	0.0230	0.0243	0.0202	0.0212
r^2	0.57	0.64	0.37	0.37	0.38
Slope (CO_2/PPFD, μmol/μmol)	0.0034	0.0066	0.0054	0.0044	0.0103
Intercept (CO_2 flux, μmol·m^{-2}·s^{-1})	−1.50	−1.16	−3.59	−0.88	−2.05
r^2	0.74	0.58	0.42	0.25	0.53

† PPFD < 500 μmol·m^{-2}·s^{-1}.

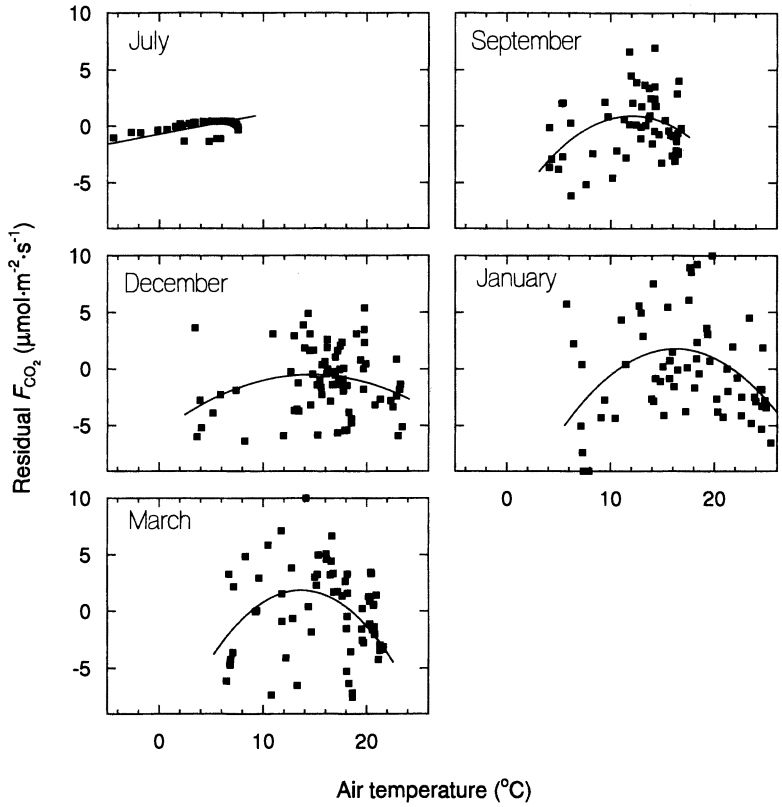

FIG. 8. Relationship between residual net ecosystem CO_2 exchange (F_{CO_2}) and air temperature (T_a) at different times of the year. The solid line shows the best-fit linear or quadratic models. For July residual (F_{CO_2}) = $0.074 \cdot T_a - 0.30$ ($P < .05$, $r^2 = 0.21$), September = $-0.1076 \cdot T_a^2 + 2.219 \cdot T_a - 9.44$ ($P < .001$, $r^2 = 0.29$), December = $-0.0363 \cdot T_a^2 + 0.751 \cdot T_a - 4.15$ ($P < .01$, $r^2 = 0.15$), January = $-0.0521 \cdot T_a^2 + 1.517 \cdot T_a - 8.52$ ($P < .01$, $r^2 = 0.22$), March = $-0.0713 \cdot T_a^2 + 1.618 \cdot T_a - 5.68$ ($P < .001$, $r^2 = 0.25$).

above-canopy PPFD (canopy quantum yield) was almost constant at ≈0.022 μmol/μmol throughout the spring and summer. In the winter, however, canopy quantum yield dropped to about a quarter of this value (Table 3). Over the course of the year, the ecosystem light compensation point varied between ≈130 and 350 $\mu mol \cdot m^{-2} \cdot s^{-1}$.

We examined the efficiency of net daytime and 24-h CO_2 uptake as a function of PPFD (Table 4). Daytime photosynthetically active photon flux use efficiencies ranged from <0.001 mol/mol in winter to almost 10 mmol/mol in late summer, averaging ≈5 mmol/mol. On a 24-h basis there was a net loss of CO_2 from the forest on our days of measurement for winter (July) to late spring (December). During mid- and late summer, 24-h photosynthetically active photon flux use efficiencies reached a maximum of ≈0.005 mol/mol. Even in the middle of the summer, however, the ecosystem was a net source of CO_2 on some days.

Temperature.—A quadratic model was used to simulate the temperature response of photosynthetic biochemistry, and explained a significant amount of the residual variation in net daytime forest CO_2 exchange after accounting for the effects of PPFD (Fig. 8) ($P <$ .05 for each of the spring and summer measurement periods). In September, 98% of the variance accounted for by the regression was associated with the second-order term, and 2% with the linear term. Approximately 33, 87, and 46% of the regression variance was associated with the second-order term in December, January, and March, respectively. In each of these cases the quadratic terms were significant ($P <$ .05). The optima for net CO_2 uptake implied by the best-fit equations (Fig. 8) increase from ≈10°C in the spring to ≈15°C in midsummer. In winter (July), however, net uptake increased linearly with temperature up to the maximum observed of ≈7°C. Our results suggested that the beech forest daytime net CO_2 exchange would become negative at temperatures above ≈30°C. At our site, temperatures exceeded this level on average only 1 d/yr.

Air saturation deficit.—The residual variation in net daytime forest CO_2 exchange after accounting for the effects of PPFD could also be associated with variations in the canopy-air saturation deficit (D) ($P < .05$ for the spring and summer measurement periods, r^2 values ranged between 0.19 and 0.34 when $D > 0.5$ kPa, Fig. 9). Net ecosystem CO_2 exchange decreased by ≈3 $\mu mol \cdot m^{-2} \cdot s^{-1} \cdot kPa^{-1}$ in late spring and early summer and by about twice this amount in early spring and late

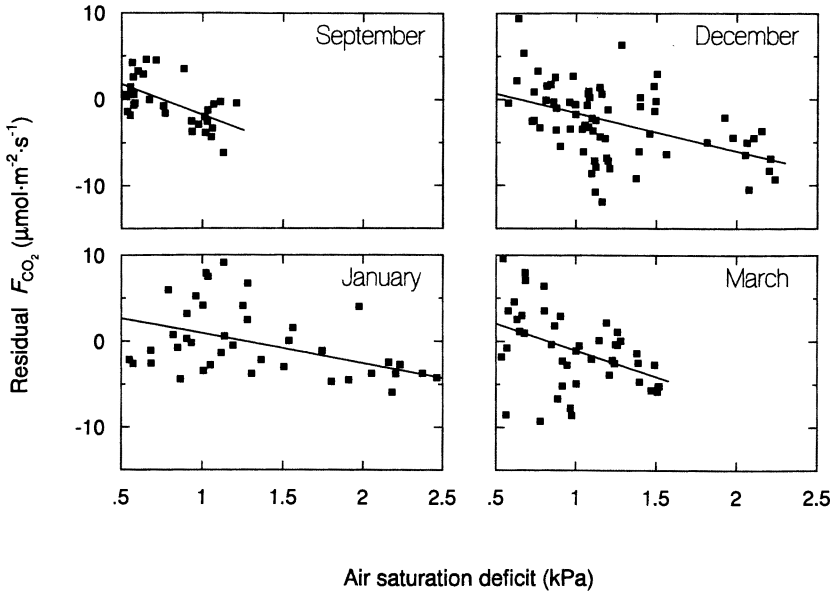

FIG. 9. Relationship between residual CO_2 flux (F_{CO_2}) and air saturation deficit (D) at different times of the year. For periods when $D > 0.5$ kPa, September residual (F_{CO_2}) = 5.28 − 7.0·D ($P < .01$, $r^2 = 0.34$), December = 2.87 − 4.47·D ($P < .01$, $r^2 = 0.21$), January = 4.86 − 3.54·D ($P < .01$, $r^2 = 0.20$), March = 6.98 − 7.71·D ($P < .01$, $r^2 = 0.22$).

summer. Maximum canopy-air saturation deficits at this site were generally <2 kPa. However, because D and air temperature were highly correlated ($0.93 < r < 0.95$ for the five measurement periods), there was no significant residual variance in CO_2 exchange associated with D after accounting for the effects of PPFD and air temperature.

Diffuse PPFD.—The efficiency of ecosystem light use (moles of CO_2 taken up per mole of photosynthetically active photons) was greater on the three overcast days of our study than on the clear days (Table 4), and total daily net ecosystem CO_2 uptake was greater despite the total PPFD on the cloudy days being from 21 to 45% lower than on the clear days. Some of the difference in net ecosystem CO_2 exchange probably resulted from the more favorable temperature and humidity conditions on the cloudy days. However, the high rates of net CO_2 uptake on these days led us to consider whether the diffuse nature of the PPFD was significant. We found that the initial slope of the relationship between predominantly (>67%) diffuse PPFD and net CO_2 exchange during cloudy periods, at 0.0152 mol/mol, was ≈50% greater than that between predominantly direct (<33% diffuse) PPFD and net CO_2 exchange at 0.0097 mol/mol ($P < .01$, $t_{91} = 2.28$). Diffuse PPFDs were moderately correlated with total PPFDs ($0.13 < r < 0.51$) and were associated with a small but significant amount of residual CO_2 exchange after accounting for total PPFD and temperature effects in the summer ($P < .05$, r^2 values of 0.07–0.13).

Influence of environmental factors on nighttime CO_2 exchange

We measured nighttime CO_2 efflux from the forest on nights with air temperatures ranging between −5° and 20°C (Fig. 10A). At air temperatures below zero respiration continued, as most biomass remained unfrozen. The 30-min CO_2 fluxes we recorded at night

TABLE 4. Relationship between CO_2 exchange and daily PPFD in a beech forest.

Date	Total PPFD (mol·m^{-2}·d^{-1})	% diffuse	Net CO_2 exchange (mol·m^{-2}·d^{-1})		CO_2 use efficiency (mol/mol)	
			Daytime	24 h	Daytime	24 h
21–23 July	19.0	19	0.016	−0.105	0.0008	
23–24 September	40.7	19	0.136	−0.078	0.0033	
25 September	22.3	84	0.162	−0.052	0.0073	
6–8 December	73.2	13	0.21	−0.082	0.0029	
19 January	47.1	33	0.41	0.26	0.0087	0.0054
20–21 January	59.5	14	0.094	−0.060	0.0016	
28 February	34.7	33	0.32	0.13	0.0092	0.0038
1–2 March	43.7	14	0.31	0.12	0.0071	0.0028

were more variable than daytime fluxes and were not well associated with either air or soil temperatures. For example, a nonlinear least-squares fit of the Arrhenius relation based on air temperature (Fig. 10A) yielded an apparent activation energy of −50 kJ/mol (with temperature coefficient, Q_{10}, of 2.0, i.e., respiration doubles with a 10°C rise in temperature) but an r^2 of only 0.08 ($P < .001$). Although the 30-min fluxes were only poorly related to temperature, mean nighttime respiration rates were clearly a function of air temperature (Fig. 10B), with an r^2 of 0.43. The apparent activation energy dropped by ≈30% to −36 kJ/mol (Q_{10} of 2.8) for the model based on nighttime mean temperatures.

On a half-hourly basis, nighttime respiration appeared to be most tightly correlated with the rate of sensible heat (warm air) exchange between the surface of the canopy and the atmosphere (Fig. 11). The component eddy and change in storage fluxes behaved inversely in response to heat flux. The eddy flux of CO_2 out of the forest increased (became more negative) with an increase in downward (negative) heat flux ($P < .01$, $r^2 = 0.44$, Fig. 11A), but that associated with changing CO_2 storage in the forest air column decreased in absolute magnitude as the mean downward heat flux increased ($P < .05$, $r^2 = 0.13$, Fig. 11B). The net effect was a lesser, but still significant, increase in ecosystem efflux (more negative CO_2 flux) with an increase in sensible heat flux delivered to the surface ($P < .01$, $r^2 = 0.21$, Fig. 11C).

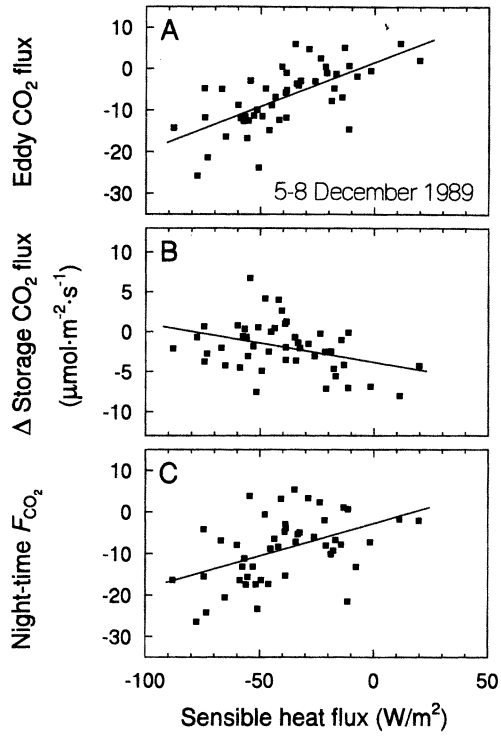

FIG. 11. Relationship between nighttime heat flux and ecosystem CO_2 exchange. (A) Eddy flux. (B) Δ-storage flux. (C) Total ecosystem respiration.

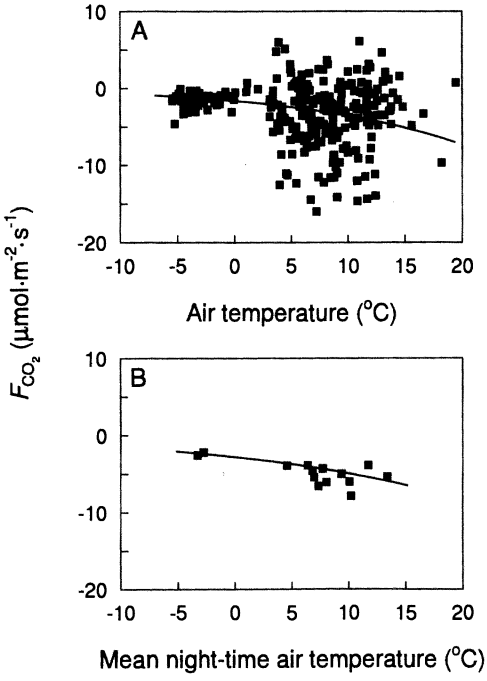

FIG. 10. Relationship between nighttime respiration and air temperature (T_a). Solid lines are best-fit Arrhenius equations. (A) Half-hourly data, $F_{CO_2} = -5.68 \cdot 10^9 \cdot e^{\{-49\,797/[8.3 \cdot (T_a + 273.1)]\}}$, $r^2 = 0.08$. (B) Mean nighttime data, $F_{CO_2} = -2.39 \cdot 10^7 \cdot e^{\{-36\,162/[8.3 \cdot (T_a + 273.1)]\}}$, $r^2 = 0.43$.

DISCUSSION

Comparison with other estimates of ecosystem CO_2 exchange

In comparison with values for ecosystem CO_2 exchange from the few previous studies, the net midday summer exchange rate of the undisturbed beech forest is low at 7–12 $\mu mol \cdot m^{-2} \cdot s^{-1}$. Midday summer values for net CO_2 exchange were ≈14 $\mu mol \cdot m^{-2} \cdot s^{-1}$ over Sitka spruce (Jarvis et al. 1976), 16–20 $\mu mol \cdot m^{-2} \cdot s^{-1}$ above second-growth oak–hickory forest (Verma et al. 1986), and 10–22 $\mu mol \cdot m^{-2} \cdot s^{-1}$ above tropical forest (Fan et al. 1990). Our data are more similar to the 8–12 $\mu mol \cdot m^{-2} \cdot s^{-1}$ measured over evergreen macchia by Valentini et al. (1991), although these values were obtained in the Mediterranean cool season. In contrast, peak CO_2 flux values over a temperate C_4 grassland reached ≈30 $\mu mol \cdot m^{-2} \cdot s^{-1}$ (Kim and Verma 1990), and for various crop species ranged between 20 and 45 $\mu mol \cdot m^{-2} \cdot s^{-1}$ (Baldocchi et al. 1981, Anderson et al. 1984, Ohtaki 1984).

The relatively low maximum rate of daytime CO_2 uptake by our beech forest results from at least two major factors. First, nighttime respiration rates were relatively high (equivalent to 40–100% of midday net CO_2 uptake rate), which would depress daytime net

TABLE 5. Summary of variation in ecosystem CO_2 exchange accounted for by several environmental factors.*

Factor	Model	Model sum of squares/total sum of squares: Winter	Early spring	Late spring	Summer	Late summer
PPFD	$P_{max}\cdot PPFD/(K_m + PPFD) - R_d$	0.77	0.75	0.67	0.41	0.56
Air temperature	$a\cdot T^2 + b\cdot T - c$	0.05	0.08	0.05	0.13	0.11
Diffuse PPFD	$d\cdot(difPPFD) - e$	†	0.01	†	0.06	0.03
Total	$[P_{max}\cdot PPFD/(K_m + PPFD)] - a\cdot T^2 + b\cdot T - d\cdot(difPPFD) - (R_d - c - e)$	0.82	0.80	0.72	0.60	0.70

* P_{max}, K_m, R_d, and $a - e$ are fitted coefficients; see *Introduction: Leaf and tissue gas exchange.*
† Clear skies during measurement period.

CO_2 uptake. This was particularly evident during the period of tree-canopy expansion in December (Fig. 6 and Table 2) when growth respiration rates were probably highest, reflecting the mobilization and use of carbohydrate reserves. Second, nutrient availability in old-growth forests is generally low. Foliar analysis and shoot gas-exchange measurements indicated that leaf nitrogen concentration and photosynthetic capacity are low in beech forest (Hollinger 1989, Köstner et al. 1992).

Summer nighttime CO_2 efflux from the beech forest was generally ≈ -5 to -7 $\mu mol\cdot m^{-2}\cdot s^{-1}$. These rates are somewhat high considering the cool nighttime temperatures at our site (average nighttime air temperature was <10°C during CO_2 flux measurements). However, our forest contained large quantities of respiratory carbon substrate in soil and forest floor litter ($\approx$200 Mg/ha; K. Tate, *personal communication*) and aboveground biomass ($\approx$180 Mg/ha; estimated after Beets 1980). Even so, nighttime ecosystem CO_2 efflux rates similar to ours were observed in a tropical forest with air temperatures of $\approx$20°C (Fan et al. 1990). The nighttime CO_2 efflux in the tropical forest was $\approx$30% of the value of the maximum daytime CO_2 uptake rate.

Equivalent-temperature nighttime respiration rates can be estimated, and such calculations are useful here. We define the temperature coefficient Q_{10} as 2 (i.e., respiration doubles with a 10°C increase in temperature) and employ the relation:

$$R_T = R_{T0}\cdot Q_{10}^{(T-T_0)/10}, \quad (9)$$

where R_T is respiration rate at a temperature T and R_{T0} is respiration rate at a second temperature T_0. Applying these calculations to the comparative forest data suggests that nighttime CO_2 efflux from the tropical forest would be equivalent to $\approx$50–70% of that in our beech forest. Equivalent-temperature nighttime CO_2 efflux rates from a temperate C_4 grassland were generally similar to our beech forest data under well-watered conditions (Kim and Verma 1990). However, at the end of a summer drought, equivalent-temperature nighttime CO_2 efflux from the grassland was only about one half of that expected from beech forest. For well-watered crops, equivalent-temperature nighttime CO_2 efflux was only $\approx$25–50% of that expected from beech forest (Anderson et al. 1984, Ohtaki 1984). Average nighttime CO_2 exchange rates of ≈ -5 $\mu mol\cdot m^{-2}\cdot s^{-1}$ from an evergreen shrub stand over three nights during the Mediterranean cool season (Valentini et al. 1991) are more comparable to our beech forest data, but temperatures were not given.

Factors regulating daytime CO_2 uptake

Light.—Our most robust result was that net daytime ecosystem CO_2 uptake was consistent with a saturating functional response to PPFD (photosynthetically active photon flux density). A saturation response to light intensity was also observed in other natural ecosystem-scale and some crop stand CO_2 exchange studies (e.g., Baldocchi et al. 1981, Anderson et al. 1984, Verma et al. 1986, Kim and Verma 1990, Fan et al. 1990, Valentini et al. 1991). There appears to be a tendency, however, for crop canopies to more nearly approach a linear response than other canopies (e.g., Denmead 1976, Anderson et al. 1984, Ohtaki 1984). This is probably a consequence of the higher PPFD levels required for light saturation in well-fertilized annual plant leaves (Field and Mooney 1986), and possibly also of a more efficient canopy architecture in plants bred to maximize production.

The relationship between net ecosystem CO_2 exchange rate and PPFD changed during the year, which may be caused by seasonal variation in the biochemistry of gas exchange (resulting from changes in leaf nutrition or ageing) or by variation in other factors that affect leaf gas exchange. For example, temperature and air saturation deficit covary with PPFD, and at certain levels at certain times of the year may depress CO_2 exchange. Such effects modify the parameters in models of the PPFD–net ecosystem CO_2 exchange relationship, and can be identified in a simultaneous nonlinear fitting of the PPFD and temperature models to the ecosystem CO_2 exchange data (e.g., Table 5). Although the model parameters shift slightly in such a fit, the essential characteristics of ecosystem CO_2 exchange (saturating with PPFD, temperature optimum, etc.) remain.

In winter (July), however, the change in the constants of our empirical models is almost certainly associated with changing leaf function. We believe that the depression in the fitted P_{max} (maximum rate of photosynthesis; Table 3) is a sign of photoinhibition resulting from the low nighttime temperatures (Table 2), because values were well below those measured 2 mo later under similar daytime conditions. The almost-linear relationship between PPFD and net ecosystem CO_2 up-

take in the winter and the depressed canopy quantum yield are consistent with photoinhibition.

Kim and Verma (1990) also observed seasonal shifts in the PPFD–net ecosystem CO_2 exchange relationship in a natural grassland. Their results suggest a decrease in the whole-canopy P_{max} and a lower saturating PPFD late in the season with the onset of senescence.

Temperature.—Our observation of an optimal temperature for net ecosystem CO_2 uptake has not been previously reported, but is an obvious consequence of the temperature response of the assimilatory and respiratory reactions that are the basis for CO_2 exchange. The optimum temperatures recorded here for ecosystem CO_2 uptake are well below those generally observed at the leaf level (Berry and Raison 1981) and are partially a consequence of the large amount of ecosystem respiratory substrate and the temperature coefficient of the respiratory reactions. However, the daytime decline in CO_2 uptake with temperatures above the optimum is greater than that expected from nighttime respiration values. Because the baseline respiration rate in the day is likely to be lower than at night (leaf dark respiration effectively disappears), it seems that the daytime decrease in net ecosystem CO_2 uptake at higher temperature may be a response to factors in addition to temperature, such as air saturation deficit (see below).

In at least one previous study (Baldocchi et al. 1981) a similar decline in the net CO_2 uptake of an alfalfa field was noted as temperatures increased above 23°C. These authors ascribed the decrease in net CO_2 uptake to enhanced root and soil respiration.

Air saturation deficit.—It is difficult to identify the independent effects of air saturation deficit (D) and air temperature on residual CO_2 flux at the scale of an ecosystem because large values of D were inevitably associated with high air temperatures. Increasing D and air temperature, however, affect forest carbon gain via different mechanisms; an increase in the air saturation deficit leads to stomatal closure and a decrease in CO_2 conductance whereas higher temperatures alone result in enhanced respiration. We calculated ecosystem surface conductance (g_s), which consists of components from the trees, epiphytes, understory, and forest floor according to the equations in Köstner et al. (1992). Most of the water flux from this forest comes from the trees (Kelliher et al. 1992) so $g_s \approx g_{canopy}$. The forest surface conductance decreased significantly with an increase in D, dropping by ≈50% when D increased from 0.5 to 1.5 kPa (Fig. 12). Leaf and tree conductance measured in the summer also decreased by ≈50% as D increased from 0.5 to 1.5 kPa (Köstner et al. 1992). At the scale of a leaf, this decrease in stomatal conductance corresponds with an ≈16% decline in *Nothofagus* photosynthesis (Hollinger 1987). We extend this calculation to the scale of a tree canopy by first approximating midday tree-canopy photosynthesis as the sum of midday CO_2 exchange and 1/2 the absolute

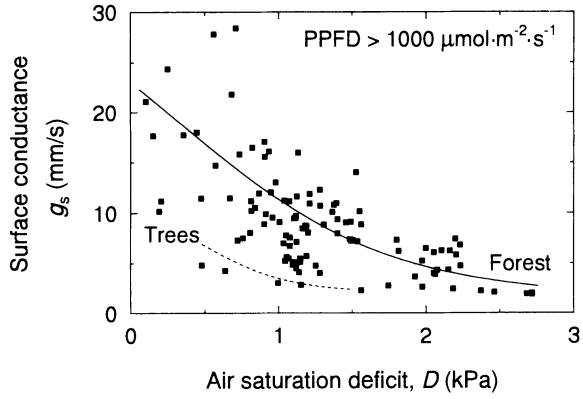

FIG. 12. Daytime summer beech forest surface conductance to water vapor. The dashed line is the best-fit relation of canopy conductance of emergent trees of the same forest to D determined by the xylem sap flow method (Köstner et al. 1992). The solid line shows the best fit for a similar relationship between forest surface conductance and D where $g_s = e^{[3.729 - 3.397 \cdot (1/(1+e^{(1.1(D - 1.445)/0.928)}))]}$, $r^2 = 0.62$. About 1/2 of total forest evaporation comes from emergent trees.

value of nighttime respiration. Assuming the same proportional change in photosynthesis with a change in conductance at the canopy level as at the leaf level, we estimate that the corresponding decrease in midday tree-canopy photosynthesis associated with a 1 kPa increase in D would be ≈1.5–2.5 $\mu mol \cdot m^{-2} \cdot s^{-1}$. However, the slope of the relationship between D and residual net ecosystem exchange rate of 3.5–7 $\mu mol \cdot m^{-2} \cdot s^{-1} \cdot kPa^{-1}$ was several times greater than this estimated effect of D, suggesting that the afternoon decline in net ecosystem CO_2 exchange rate (Fig. 6) was partly (≈40%) caused by D and partly (≈60%) by enhanced respiration due to higher temperatures. A decrease in net ecosystem CO_2 uptake with increasing D has been previously observed over Sitka spruce (Jarvis et al. 1976) and a natural grassland (Kim and Verma 1990), but not over a second-growth oak–hickory forest (Verma et al. 1986) and does not appear to be typical of crop canopies.

Diffuse light.—Price and Black (1990) also observed enhanced forest CO_2 uptake on overcast days. We suggest that the enhancement of net ecosystem CO_2 uptake by isotropic light derives from the efficient penetration of such radiation through the canopy. Ross (1981) modeled the penetration of radiation through canopies consisting of randomly dispersed leaves of various orientations and found that a greater proportion of diffuse sky radiation penetrates to depth within a canopy than does solar beam radiation. Sheehy and Chapas (1976) found that the PPFD within a canopy was a higher proportion of the incident above-canopy PPFD during overcast (diffuse) conditions than during clear conditions, a result also obtained at the shoot (Oker-Blom 1985) and canopy (Jarvis et al. 1985) levels in simulation studies. Because of the nonlinearity in the light–photosynthesis relationship, a more even distribution

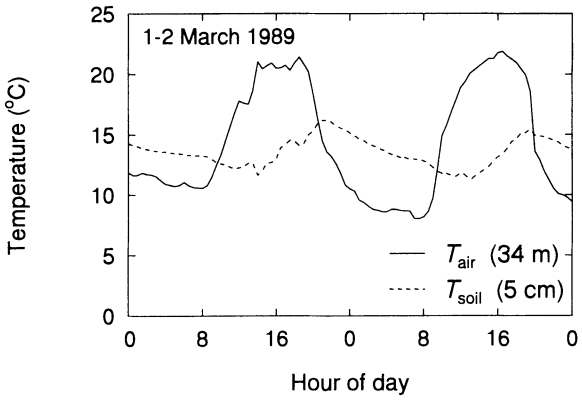

FIG. 13. Diurnal pattern of air and soil temperatures at the forest site. Soil temperature at 5 cm depth lagged about 4 h behind air temperature.

of radiation through a canopy will enhance total photosynthetic production (Verhaggen et al. 1963). This result has been previously confirmed at the shoot level (Zelawski et al. 1973, Oker-Blom 1985).

Based on a light–CO_2 relationship similar to that observed in our study, Fan et al. (1990) speculated that an increase in cloudiness might decrease net ecosystem CO_2 uptake in a tropical forest. Our results show that this may not be true. Although cloudiness generally lowers the PPFD, which leads to decreased ecosystem CO_2 uptake, the coincident effect of increasing the diffuse fraction of the total PPFD pushes ecosystem CO_2 uptake in the opposite direction. Although net ecosystem CO_2 uptake would probably decrease with heavy cloud, we found that net CO_2 uptake can increase with hazy or moderately cloudy skies (Table 4).

The response of ecosystem CO_2 uptake to diffuse PPFD may already be of global consequence. The general level of haze in much of the northern temperate zone has increased over the last 40 yr (e.g., Husar and Patterson 1986). If other ecosystems behave similarly to the New Zealand beech forest, the increase in haze and consequent ecosystem response may be partly responsible for the enhanced terrestrial CO_2 sink postulated for the northern temperate zone (Tans et al. 1990). Should this be true, however, efforts to reduce haze-producing aerosols might ultimately reduce terrestrial biosphere CO_2 uptake.

Turbulent mixing.—During daylight hours, there was no relationship between turbulent mixing as determined by either the horizontal windspeed u, or the friction velocity, U^* ($\overline{w'u'}^{0.5}$) and net ecosystem CO_2 exchange. However, other workers have shown that crop canopy CO_2 exchange can decrease at very low wind speeds (Baldocchi et al. 1981, Ohtaki 1984), concluding that the CO_2 flux to the leaf surfaces was inhibited at very low wind speeds, which resulted in a localized CO_2 depletion and a consequent reduction in photosynthesis. This daytime stagnation of airflow is less likely in the rough canopy of a forest. Baldocchi et al. (1981) also suggested that the movement induced in crop canopies at higher wind speeds promoted greater penetration of radiation to the lower, non-light-saturated layers of the canopy, increasing total photosynthesis.

Summary of factors regulating daytime CO_2 uptake.—Most of the variation in daytime half-hourly forest CO_2 exchange can be accounted for by simple models that emulate the leaf-level responses of photosynthesis to light and temperature (Table 5). Incorporating a positive effect due to diffuse PPFD results in a slight (but significant) additional improvement (Table 5). There is no significant stepwise improvement when considering the air saturation deficit because the influence of this factor is incorporated in the quadratic temperature response. The residual variation consists of measurement error and other (possibly biological) components. One of these components may be variation in CO_2 sink strength across the forest. Because of shifts in wind speed and direction, we measured the CO_2 exchange of forest patches that changed in size and location around our tower. Such variation could be evaluated in future studies.

Environmental factors affecting nighttime respiration

The Arrhenius model of respiration (Eq. 4) accounted for $<10\%$ of variation in the relationship between 30-min averages of nighttime ecosystem CO_2 efflux rate and air temperature, although at the scale of a leaf, the model has generally been successful in describing variation in dark respiration rates measured under steady-state conditions in chambers (e.g., Berry and Raison 1981). There are at least two possible reasons for the failure of the theoretical model to explain the results of CO_2 efflux measurements made under natural conditions at the scale of an ecosystem.

First, all components of the ecosystem respire at night—leaves, stems, boles, roots, and heterotrophs throughout the soil profile. In a 30-m-tall forest, there was inevitably some variation in temperature, even at night. This variation was partly due to phase differences in the daily courses of the temperature of different ecosystem components. For example, air temperature measured above the forest on a fine summer day varied by ≈ 15°C, with a minimum obtained just before dawn and a maximum reached late in the afternoon (Fig. 13). At a depth of 0.05 m in the soil, the corresponding diurnal temperature amplitude was generally reduced by $\approx 70\%$, and maximum and minimum temperatures were lagged by ≈ 7 h (Fig. 13). With increasing depth in the soil, the diurnal temperature amplitude decreased and the phase lag increased (data not shown). This problem of the temperature of different compartments lagging one another disappears with an average taken over the entire night.

A second, apparently more important, factor contributing to variability in nighttime CO_2 efflux rate

relates to the dynamics of nighttime turbulent mixing between the atmosphere and ecosystem (Fitzjarrald and Moore 1990). The combination of radiative cooling and tendency to low wind speeds on clear nights promotes development of a stratified air layer above the tree canopy that "traps" CO_2 in the forest. Periodically, large-scale turbulent episodes associated with occasional increases in nocturnal wind speed appear to enhance vertical mixing, transporting sensible heat down to the canopy and allowing CO_2 in the forest to "escape." There are at least three possible mechanisms for generating turbulence episodes on clear nights. At our site, they may be attributable to large-scale variation in airflow over irregular regional topography. At a flat, extensive rain forest site, nighttime turbulence was postulated to be associated with an irregular, nocturnal jet stream appearing 4–8 times per night (Fitzjarrald and Moore 1990). A third explanation involves turbulence triggered by the passage of gravity waves (large-scale variations in atmospheric density; Nappo 1991).

Our strong positive relationship between nighttime CO_2 efflux and downward sensible heat flux density (Fig. 11) is consistent with CO_2 exchange being regulated by periodic turbulence episodes. So too was our inverse relationship between CO_2 concentration in the forest air column and downward sensible heat flux density. Although the rate of production of CO_2 is ultimately regulated by the temperature, mass, and quality of the respiratory substrate, CO_2 efflux rates were controlled by intermittent transport processes that apparently occurred at a frequency of the same order as our 30-min measurement integration period.

Conclusions

In an undisturbed old-growth forest, net daytime CO_2 uptake was low and nighttime respiration rates were relatively high, and both at least partly result from the high quantities of organic matter in the forest.

In many significant ways the CO_2 exchange patterns of this forest were similar to the patterns observed at the leaf level and that are the direct result of the kinetics of leaf biochemistry. These similarities include the saturating response of net ecosystem CO_2 uptake to PPFD, the response of uptake to temperature and air saturation deficit, and the winter observation of apparent photoinhibition. This suggests that the prospects of scaling-up biochemically based models of leaf gas exchange for simulating ecosystem CO_2 exchange should be excellent.

The seasonal change in the kinetic parameters of the PPFD–CO_2 uptake relationship and the changing rate of temperature-adjusted nighttime respiration are evidence that biological and ecological factors may modify the influence of the environmental factors of light, temperature, and air saturation deficit. Net ecosystem CO_2 exchange also responded to changing physical characteristics that are of little importance at the level of leaf biochemistry, such as the spatial distribution of above-canopy PPFD, and the episodic nature of nocturnal turbulent transport.

Therefore, although an understanding of leaf-level biology is fundamental to interpreting ecosystem CO_2 exchange patterns, this must be coupled with information on the ecology of the system and the physics of radiation and turbulent transport before an interpretation of ecosystem CO_2 exchange can be complete.

Acknowledgments

We wish to thank D. Baldocchi, R. McMillen, and other researchers at the NOAA Atmospheric Turbulence and Diffusion Division for their support and encouragement in using the eddy-correlation technique. We thank also J. Orwin for her valuable comments on the manuscript. This work was supported by funding from the New Zealand Foundation for Research, Science, & Technology and the New Zealand Department of Conservation.

Literature Cited

Anderson, D. E., and S. B. Verma. 1985. Turbulence spectra of CO_2, water vapor, temperature, and wind velocity fluctuations over a crop surface. Boundary-layer Meteorology **33**:1–14.

Anderson, D. E., S. B. Verma, and R. J. Clement. 1986. Turbulence spectra of CO_2, water vapor, temperature and velocity over a deciduous forest. Agricultural and Forest Meteorology **38**:81–99.

Anderson, D. E., S. B. Verma, and N. J. Rosenberg. 1984. Eddy correlation measurements of CO_2, latent heat, and sensible heat fluxes over a crop surface. Boundary-layer Meteorology **29**:263–272.

Baldocchi, D. D., B. B. Hicks, and T. P. Meyers. 1988. Measuring biosphere–atmosphere exchanges of biologically related gases with micrometeorological methods. Ecology **69**: 1331–1340.

Baldocchi, D. D., S. B. Verma, and N. J. Rosenberg. 1981. Environmental effects on the CO_2 flux and CO_2–water flux ratio of alfalfa. Agricultural Meteorology **24**:175–184.

Beets, P. N. 1980. Amount and distribution of dry matter in a mature Beech/Podocarp community. New Zealand Journal of Forestry Science **10**:395–418.

Berry, J. A., and J. K. Raison. 1981. Responses of macrophytes to temperature. Pages 277–338 *in* O. L. Lange, P. S. Nobel, C. B. Osmond, and H. Ziegler, editors. Physiological plant ecology. Volume 12A. Responses to the physical environment. Springer-Verlag, New York, New York, USA.

Businger, J. A., and A. C. Delany. 1990. Chemical sensor resolution required for measuring surface fluxes by three common micrometeorological techniques. Journal of Atmospheric Chemistry **10**:399–410.

Carter, G. C., and J. F. Ferrie. 1979. A coherence and cross spectral estimation program. Pages 2.3-1 to 2.3-18 *in* Digital Processing Committee, editors. Programs for digital signal processing. IEEE Press, New York, New York, USA.

Collatz, G. J., J. T. Ball, C. Grivet, and J. A. Berry. 1991. Physiological and environmental regulation of stomatal conductance, photosynthesis and transpiration: a model that includes a laminar boundary layer. Agricultural and Forest Meteorology **54**:107–136.

Denmead, O. T. 1976. Temperate cereals. Pages 1–31 *in* J. L. Monteith, editor. Vegetation and the atmosphere. Volume 2. Case studies. Academic Press, London, England.

Dyer, A., B. B. Hicks, and K. M. King. 1967. The fluxatron—a revised approach to the measurement of eddy fluxes in the lower atmosphere. Journal of Applied Meteorology **6**:408–413.

Fan, S.-M., S. C. Wofsy, P. S. Bakwin, D. J. Jacob, and D. R. Fitzjarrald. 1990. Atmosphere–biosphere exchange of CO_2 and O_3 in the central Amazon forest. Journal of Geophysical Research **95(D10)**:16851–16864.

Farquhar, G. D., S. von Caemerrer, and J. A. Berry. 1980. A biochemical model of photosynthetic CO_2 assimilation in leaves of C_3 plants. Planta **149**:78–90.

Field, C., and H. A. Mooney. 1986. The photosynthesis–nitrogen relationship in wild plants. Pages 25–55 *in* T. J. Givnish, editor. On the economy of plant form and function. Cambridge University Press, Cambridge, England.

Fitzjarrald, D. R., and K. E. Moore. 1990. Mechanisms of nocturnal exchange between the rain forest and the atmosphere. Journal of Geophysical Research **95(D10)**:16839–16850.

Hollinger, D. Y. 1987. Gas exchange and dry matter allocation responses to elevation of atmospheric CO_2 concentration in seedlings of three tree species. Tree Physiology **3**:193–202.

———. 1989. Canopy organization and foliage photosynthetic capacity in a broad-leaved evergreen montane forest. Functional Ecology **3**:53–62.

Husar, R. B., and D. E. Patterson. 1986. Haze climate of the United States. EPA/600/3-86/071. Atmospheric Studies Research Laboratory, United States Environmental Protection Agency, Research Triangle Park, North Carolina, USA.

Jarvis, P. G., G. B. James, and J. J. Landsberg. 1976. Coniferous forest. Pages 171–240 *in* J. L. Monteith, editor. Vegetation and the atmosphere. Volume 2. Case studies. Academic Press, London, England.

Jarvis, P. G., H. S. Miranda, and R. I. Muetzelfeldt. 1985. Modelling canopy exchanges of water vapor and carbon dioxide in coniferous forest plantations. Pages 521–543 *in* B. A. Hutchison and B. B. Hicks, editors. The forest–atmosphere interaction. D. Reichel, Dordrecht, The Netherlands.

Kaimal, J. C., J. C. Wyngaard, Y. Izumi, and O. R. Coté. 1972. Spectral characteristics of surface-layer turbulence. Quarterly Journal of the Royal Meteorological Society **98**: 563–589.

Kelliher, F. M., B. M. Köstner, D. Y. Hollinger, J. N. Byers, J. E. Hunt, T. M. McSeveny, M. Meserth, P. L. Weir, and E.-D. Schulze. 1992. Evaporation, xylem sap flow, and tree transpiration in a New Zealand broad-leaved forest. Agricultural and Forest Meteorology **62**:53–73.

Kim, J., and S. B. Verma. 1990. Carbon dioxide exchange in a temperate grassland ecosystem. Boundary-layer Meteorology **52**:135–149.

Kirchbaum, M. U. F., and G. D. Farquhar. 1984. Temperature dependence of whole-leaf photosynthesis in *Eucalyptus pauciflora* Sieb. ex Spreng. Australian Journal of Plant Physiology **11**:519–538.

Köstner, B. M., E.-D. Schulze, F. M. Kelliher, D. Y. Hollinger, J. N. Byers, J. E. Hunt, T. M. McSeveny, M. Meserth, and P. L. Weir. 1992. Transpiration and canopy conductance in a pristine broad-leaved forest of *Nothofagus*: an analysis of xylem sap flow and eddy correlation measurements. Oecologia **91**:350–359.

Landsberg, J. J. 1977. Some useful equations for biological studies. Experimental Agriculture **13**:273–286.

Leuning, R., and J. Moncrieff. 1990. Eddy-covariance CO_2 flux measurements using open- and closed-path CO_2 analysers: corrections for analyser water vapour sensitivity and damping of fluctuations in air sampling tubes. Boundary-layer Meteorology **53**:63–76.

McBean, G. A., and M. Miyake. 1972. Turbulent transfer mechanisms in the atmospheric surface layer. Quarterly Journal of the Royal Meteorological Society **98**:383–398.

McMillen, R. T. 1988. An eddy correlation technique with extended applicability to non-simple terrain. Boundary-layer Meteorology **43**:231–245.

Moore, C. J. 1986. Frequency response corrections for eddy correlation systems. Boundary-layer Meteorology **37**:17–35.

Morison, J. I. L. 1987. Intercellular CO_2 concentration and stomatal response to CO_2. Pages 229–251 *in* E. Zeiger, G. D. Farquhar, and I. R. Cowan, editors. Stomatal function. Stanford University Press, Stanford, California, USA.

Nappo, C. J. 1991. Sporadic breakdowns of stability in the PBL over simple and complex terrain. Boundary-layer Meteorology **54**:69–87.

Ohtaki, E. 1984. Application of an infrared carbon dioxide and humidity instrument to studies of turbulent transport. Boundary-layer Meteorology **29**:85–107.

———. 1985. On the similarity in atmospheric fluctuations of carbon dioxide, water vapor and temperature over vegetated fields. Boundary-layer Meteorology **32**:25–37.

Oker-Blom, P. 1985. Photosynthesis of a Scots pine shoot: simulation of the irradiance distribution and photosynthesis of a shoot in different radiation fields. Agricultural and Forest Meteorology **34**:31–40.

Price, D. T., and T. A. Black. 1990. Effects of short-term variation in weather on diurnal canopy CO_2 flux and evapotranspiration of a juvenile Douglas-fir stand. Agricultural and Forest Meteorology **50**:139–158.

Ross, J. 1981. The radiation regime and architecture of plant stands. Dr. W. Junk Publishers, The Hague, The Netherlands.

Schmid, H. P., and T. R. Oke. 1990. A model to estimate the source area contributing to turbulent exchange in the surface layer over patchy terrain. Quarterly Journal of the Royal Meteorological Society **116**:965–988.

Schulze, E.-D. 1986. Carbon dioxide and water vapor exchange in response to drought in the atmosphere and in the soil. Annual Review of Plant Physiology **37**:247–274.

Sheehy, J. E., and L. C. Chapas. 1976. The measurement and distribution of irradiance in clear and overcast conditions in four temperate forage grass canopies. Journal of Applied Ecology **13**:831–840.

Stewart, G. H., and A. B. Rose. 1990. The significance of life history strategies in the developmental history of mixed beech (*Nothofagus*) forests, New Zealand. Vegetatio **87**:101–114.

Stewart, G. H., A. B. Rose, and T. T. Veblen. 1991. Forest development in canopy gaps in old-growth beech (*Nothofagus*) forests, New Zealand. Journal of Vegetation Science **2**:679–690.

Tans, P. P., I. Y. Fung, and T. Takahashi. 1990. Observational constraints on the global atmospheric CO_2 budget. Science **247**:1431–1438.

Valentini, R., G. E. Scarascia Mugnozza, P. De Angelis, and R. Bimbi. 1991. An experimental test of the eddy correlation technique over a Mediterranean macchia canopy. Plant, Cell and Environment **14**:987–994.

Verhaggen, A. M. W., J. H. Wilson, and E. J. Britten. 1963. Plant production in relation to foliage illumination. Annals of Botany **27**:627–640.

Verma, S. B., D. D. Baldocchi, D. E. Anderson, D. R. Matt, and R. J. Clement. 1986. Eddy fluxes of CO_2, water vapor, and sensible heat over a deciduous forest. Boundary-layer Meteorology **36**:71–91.

Webb, E. K., G. I. Pearman, and R. Leuning. 1980. Correction of flux measurements for density effects due to heat and water vapor transfer. Quarterly Journal of the Royal Meteorological Society **106**:85–100.

Wesely, M. L., and R. L. Hart. 1985. Variability of short term eddy correlation estimates of mass exchange. Pages 591–612 *in* B. A. Hutchison and B. B. Hicks, editors. The forest–atmosphere interaction. D. Reidel, Dordrecht, The Netherlands.

Zelawski, W., R. Szaniawski, W. Dybczynski, and A. Piechurowski. 1973. Photosynthetic capacity of conifers in diffuse light of high illuminance. Photosynthetica **7**:351–357.

Literature Cited

Measuring Biosphere-Atmosphere Exchanges of Biologically Related Gases with Micrometeorological Methods

Dennis D. Baldocchi; Bruce B. Hincks; Tilden P. Meyers

Ecology, Vol. 69, No. 5. (Oct., 1988), pp. 1331-1340.

Stable URL:

http://links.jstor.org/sici?sici=0012-9658%28198810%2969%3A5%3C1331%3AMBEOBR%3E2.0.CO%3B2-T

Canopy Organization and Foliage Photosynthetic Capacity in a Broad-Leaved Evergreen Montane Forest

D. Y. Hollinger

Functional Ecology, Vol. 3, No. 1. (1989), pp. 53-62.

Stable URL:

http://links.jstor.org/sici?sici=0269-8463%281989%293%3A1%3C53%3ACOAFPC%3E2.0.CO%3B2-E

The Measurement and Distribution of Irradiance in Clear and Overcast Conditions in Four Temperate Forage Grass Canopies

J. E. Sheehy; L. C. Chapas

The Journal of Applied Ecology, Vol. 13, No. 3. (Dec., 1976), pp. 831-840.

Stable URL:

http://links.jstor.org/sici?sici=0021-8901%28197612%2913%3A3%3C831%3ATMADOI%3E2.0.CO%3B2-E